

Feature Screening in Large Scale Cluster Analysis

TRAMBAK BANERJEE, GOURAB MUKHERJEE AND PETER RADCHENKO

University of Southern California

Abstract

We propose a novel methodology for feature screening in clustering massive datasets, in which both the number of features and the number of observations can potentially be very large. Taking advantage of a fusion penalization based convex clustering criterion, we propose a very fast screening procedure that efficiently discards non-informative features by first computing a clustering score corresponding to the clustering tree constructed for each feature, and then thresholding the resulting values. We provide theoretical support for our approach by establishing uniform non-asymptotic bounds on the clustering scores of the “noise” features. These bounds imply perfect screening of non-informative features with high probability and are derived via careful analysis of the empirical processes corresponding to the clustering trees that are constructed for each of the features by the associated clustering procedure. Through extensive simulation experiments we compare the performance of our proposed method with other screening approaches, popularly used in cluster analysis, and obtain encouraging results. We demonstrate empirically that our method is applicable to cluster analysis of big datasets arising in single-cell gene expression studies.

Some key words: Convex clustering; Non-asymptotic screening rate; Modality detection; High-dimensionality; Empirical Processes; Single-cell biology; RNA-Seq data

1 Introduction

We consider the problem of feature screening in large scale cluster analysis. Clustering is one of the most popular unsupervised classification techniques and is widely used in a

myriad of statistical applications for stratification and sub-population identification ([Hartigan & Wong, 1979](#); [Farcomeni & Greco, 2016](#); [Rousseeuw & Kaufman, 1990](#)). In recent years, due to massive advancements in the modern data collection and assimilation techniques, very big datasets, with both a large number of observations and a large number of features, have been generated with increasing frequency. Classical clustering methods (see, for example, Chapter 14 of [Friedman et al., 2001](#)) are either computationally challenging or ineffective for conducting segmentation analysis of such massive modern data. In many scientific applications, when the dimension of the data is very high, most of the coordinates (i.e. features) contain very little information regarding the grouping structure. Classical clustering methods, which do not reduce the dimension of the data, suffer, because the agglomerative effects of the large number of “noise” features conceal important clustering information available in a relatively smaller number of “signal” features. Recently developed clustering algorithms, such as [Witten & Tibshirani \(2012\)](#); [Arias-Castro & Verzelen \(2014\)](#); [Chan & Hall \(2012\)](#); [Jin & Wang \(2014\)](#), which exploit the underlying sparseness, are effective in dealing with high-dimensional data. Herein we propose a scalable computationally efficient approach, entitled COSCI (CONvex Screening for Cluster Information), that can efficiently weed out the features that are non-informative for clustering. As a non-parametric approach, COSCI has competitive advantages over the popular Gaussian mixture based parametric techniques ([Arias-Castro & Verzelen, 2014](#); [Azizyan et al., 2013](#)). Unlike the non-parametric density estimation based screening techniques, COSCI is very scalable, and can successfully handle datasets with more than one million observations. Our proposed procedure discards non-informative features by first computing a clustering score for the clustering tree constructed for each feature, and then thresholding the resulting values. We provide the theoretical motivation for our approach by establishing uniform non-asymptotic bounds on the clustering scores of the noise features.

Our theoretical results are a significant extension of the univariate results in [Radchenko & Mukherjee \(2014\)](#). Herein, we rely on a more careful analysis of the empirical processes corresponding to the clustering trees constructed for each feature by the associated clustering procedure. We derive a stronger tail probability bound for the clustering score of each feature, which then allows us to establish a uniform bound for all the clustering scores of the non-informative features in the high-dimensional setting, where the number of such features can be extremely large. Using this uniform bound, we infer that under mild regu-

larity conditions on the population distribution the proposed COSCI algorithm will discard the non-informative features and perfectly select the informative features with very high probability.

High dimensional datasets arising in modern biology, econometrics, engineering, text mining and signal processing (James et al., 2013) require a significant degree of feature screening for subsequent application of a clustering algorithm. We illustrate the applicability of COSCI for making scientific discoveries through the analysis of single cell biological data. Emerging technologies, such as single-cell Mass cytometry (Bendall et al., 2011), next-generation sequencing (Liu et al., 2012) and micro-fluidic methods (Dalerba et al., 2011; White et al., 2011), have recently enabled us to collect gene and protein expression information for each cell (Wang & Bodovitz, 2010). The resulting datasets, which are not only very high-dimensional but also contain a large number of cellular observations, serve as invaluable resources for the characterization of the cellular hierarchy in multi-cellular organisms. Often, the biological question associated with these datasets is the identification of homogeneous cellular sub-populations based on the differential expression patterns of the genes. The composition of these sub-populations is subsequently analyzed to detect interesting structures. Recently, several algorithms such as SPADE (Qiu et al., 2011), viSNE (Amir et al., 2013), Wanderlust (Bendall et al., 2014), Scaffold maps (Spitzer et al., 2015), SLIDE (Sen et al., 2015) and ECLAIR (Giecold et al., 2016) have been developed for conducting such sub-population analysis for single cell data. Most of these methods conduct either dimension reduction through PCA related methods or handle large sample sizes via down-sampling. While these algorithms are widely used, they lack appropriate mathematical guarantees to show that the resulting sub-populations are not due to random fluctuations and will be reproducible across datasets generated from experiments conducted under similar conditions. Furthermore, the use of techniques such as PCA to reduce dimensionality in these settings can be called into question (Chang, 1983) because (a) the inferred sub-populations may not be sparse in the expression patterns of the genes, in which case PCA has been theoretically proven to produce inconsistent results (Johnstone & Lu, 2009), (b) there is no guarantee that cluster information is aligned in the direction of maximum variance. As a motivational example, consider the problem of cellular sub-population detection in a single-cell RNAseq data that was analyzed in Giecold et al. (2016) (henceforth referred to as G16). This massive dataset holds the expression

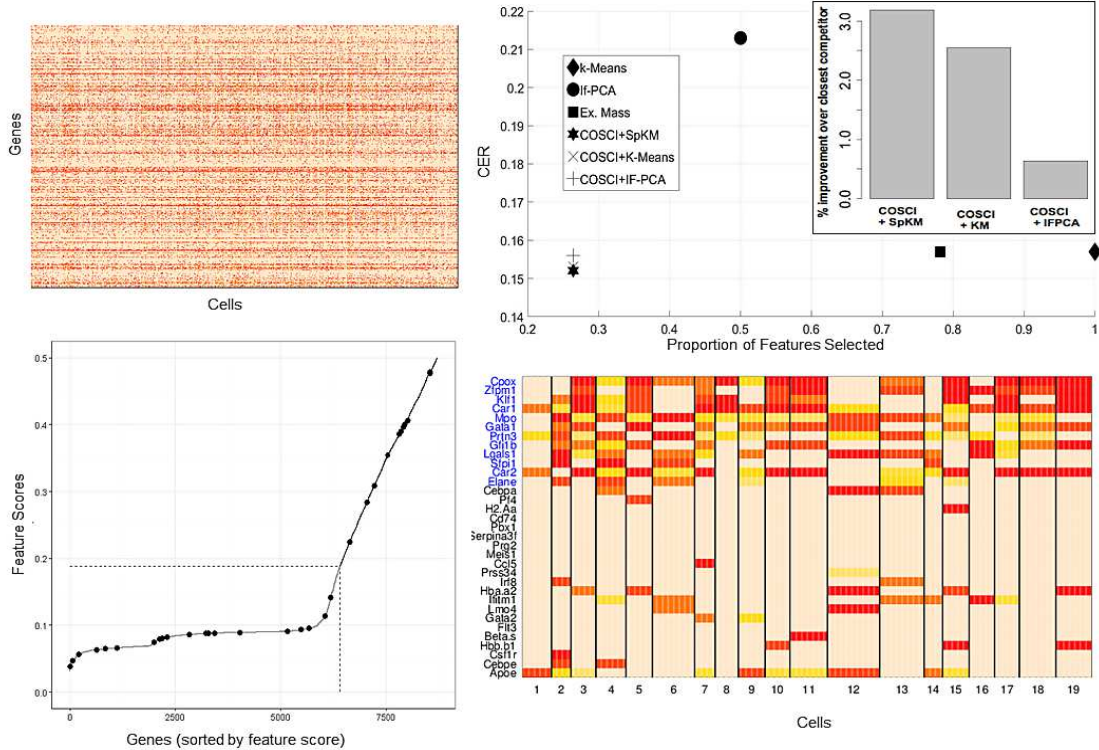


Figure 1: APPLICATION OF COSCI TO RNA-SEQ DATA OF G16. At top left we have the heatmap of the 8716×2730 expression matrix, where red denotes high expression and bisque stands for low expression. A priori we know that there are 19 sub-populations among the cells. The goal is to detect these sub-populations and study their composition with respect to the 33 lineage markers. The plot at bottom left shows the distribution of feature scores S_j . The dashed horizontal line is the screening threshold of 0.188, which is chosen by COSCI. All the features with scores above the threshold are selected. The black dots are the 33 lineage markers. The heatmap at the bottom right shows the composition of the 19 cellular sub-populations among the 33 lineage markers. The 12 lineage markers in blue are the selected ones. At top right is the plot of the error rate (y-axis) vs. the proportion of features selected (x-axis) for different methods. COSCI selects the fewest features and applying k -means or Sparse k -means to the COSCI selected features returns a smaller error rate.

levels of $p = 8716$ genes for $n = 2730$ mice bone marrow cells (Paul et al., 2015), and one of the key scientific objectives is to infer the lineage pattern of the identified sub-populations based on 33 lineage markers. If the sub-populations differ with respect to a relatively small subset of all the genes considered, then, from the statistical perspective, the problem reduces to screening out the non-informative features from the data consisting of vectors $X_j \in R^n$, $j = 1, 2, \dots, p$ and identifying a subset of features that retains the

cluster information. As such, identifying the best subset of the genes with respect to the cluster information is an important statistical endeavor with critical biological implications (Witten & Tibshirani, 2012 and the references therein).

Unlike the methods that use downsampling, COSCI can accommodate sample sizes on the order of 10^6 . COSCI first produces a score, $S_j \in (0, 0.5]$, for each feature, which reflects its relative importance for clustering, and then screens out the features with lower scores. When applied to the aforementioned RNASeq data, COSCI orders the scores of the 8716 genes and selects the top 2304 genes, which include 12 of the 33 lineage markers (see Figure 1, bottom left; the selected genes are highlighted in solid black and the black dots are the 33 lineage markers). The heatmap (Figure 1, bottom right) of the expressions for the 19 sub-populations detected via k -means on the COSCI selected features shows that the inferred sub-populations differ significantly across the 12 selected lineage markers. After applying k -means to detect the sub-populations on the 2304 genes selected by COSCI we got a misclassification error (computed as $\text{CER} = 1 - \text{Rand Index}$, Rand, 1971; Chipman & Tibshirani, 2006) of approximately 0.15. This error is significantly smaller than several other methods that are widely used for such clustering problems especially when the proportion of selected features is taken into account (see Figure 1, top right). We revisit this example with more details in Section 4.2.

1.1 Connections to Related Statistical Literature

Within the statistical literature, a number of recently proposed clustering approaches execute feature screening as the first step and then rely on conventional clustering techniques, such as k -means, to cluster the remaining data. For example, Chan & Hall (2012) proposed a non-parametric feature screening method that is based on coordinate-wise Excess Mass tests [(Cheng & Hall, 1998)]. They rank the features using the values of the corresponding test statistic. Feature selection then follows by identifying a kink in the plot of the within cluster sum of squares versus the number of identified clusters. Witten & Tibshirani (2012) proposed the Sparse k -means and Sparse Hierarchical clustering approaches, which employ k -means and hierarchical clustering, respectively, on a feature weighted dissimilarity matrix, where the weights are encouraged to be sparse. Their method is largely inspired by the popular COSA algorithm of Friedman & Meulman (2004) and is more adept at sparse clustering. Recently, Arias-Castro & Pu (2016) proposed Sparse Alternate Sum

(SAS) clustering, which uses a hill-climbing approach to solve the sparse k -means optimization problem. On the parametric side, several model based clustering approaches have been introduced (Pan & Shen (2007), Wang & Zhu (2008), Xie et al. (2008)). These techniques typically maximize a penalized likelihood under a Gaussian mixture model, where the penalization serves the purpose of implicit feature selection. Jin & Wang (2014) and Jin et al. (2015) propose IF-PCA, which is a two step clustering method - the first step conducts coordinate wise feature selection, and the second step performs k -means clustering on the matrix of left singular vectors of the selected features. The feature selection step uses the Kolmogorov-Smirnov test for Normality to rank the features, followed by the use of the Higher Criticism (HC) (Donoho & Jin, 2004, 2008) functional to finally select the features. Theoretical properties of clustering algorithms that combine feature selection with clustering have also been recently studied. For example, Azizyan et al. (2013) provide information theoretic bounds on clustering accuracy of the high dimensional Gaussian mixtures, while Arias-Castro & Verzelen (2014) establish minimax rates for the problems of mixture detection and feature selection under the sparsity assumption.

Our work is closer to the approaches of Witten & Tibshirani (2012), Jin & Wang (2014) and Chan & Hall (2012), where the objective is to screen out the noise features. We analyze the problem of feature screening in large scale clustering and propose COSCI - a novel computationally efficient screening procedure with strong theoretical motivation. COSCI uses a non-parametric approach to rank order the features by their clustering leverage. In this respect, it differs from the recently proposed screening techniques, such as IF-PCA, which rely on a parametric family as a point of reference to gauge feature strength for clustering.

1.2 Organization of the Paper

In Section 2 we present and discuss our screening methodology. More specifically, Algorithm 1 provides the details of the implementation, while Section 2.1 contains the main theoretical motivation and associated results. Section 3 provides two approaches that aid the selection of the screening threshold. In Section 4 we conduct a detailed empirical analysis of our approach using both simulated data and real data from microarray experiments. Section 5 concludes the paper. Proofs and additional technical details are relegated to the Appendix.

2 Methodology and Main Results

We consider the problem of clustering n observations based on p features under the prior information that a high proportion of these p features contain no clustering information. Noting that these “noise” features have unimodal marginal distributions (which may differ across the features), we develop a univariate approach, which, based on the sample observations, can determine if the underlying true density is unimodal. As there are many noise features, this detection of unimodality in the marginal distributions has to be conducted with very high precision. Also, features containing relevant cluster information have to possess non unimodal marginal population distribution lest they get screened out as noise by the aforementioned approach. In most practical examples, it is possible to accommodate the last requirement by considering linear combinations of features (pairwise linear combinations being the simplest case), which can then be examined for multimodality. We expect that marginally uninformative features containing correlated sub-population level information will be revealed through multi-modality of their linear combinations (see Section 4.3 for further details). However, these linear combinations increase the inherent dimensionality of the problem. For example, if we consider a fixed number of linear combinations for each pair of the original p features, we end up having to examine on the order of p^2 new features. In this case, we leverage the scalability of our proposed marginal approach. Theorem 1, provided below, shows that the marginal screening method can be accurately used even in setups where p is exponentially large with respect to n .

Our methodology is formalized in Algorithm 1 below. See Appendix 6.8 for a detailed description of the computational steps involved in Algorithm 1.

ALGORITHM 1: COSCI procedure for feature screening

INPUT: data matrix $X_{n \times p}$ and tuning parameter α_0

FOR each $j \in \{1, \dots, p\}$:

INITIALIZE:

Sort data in ascending order and store them as $x = \{x_1, \dots, x_n\}$.

Set k , the number of clusters, equal to n . For each i in $1, \dots, n$, set $c_i = \{x_i\}$.

REPEAT:

1. *Convex Merging Algorithm:*

Find consecutive adjacent centroid distances: $d(r, r+1) \leftarrow (c_{r+1} - c_r) / (|c_r| + |c_{r+1}|)$.

Find clusters with minimum merging distance: $r^* \leftarrow \arg \min_r d(r, r + 1)$.

Merge clusters r^* , $r^* + 1$, re-label remaining clusters and set $k \leftarrow k - 1$.

2. Merge Size:

Find the merge size, α_i^j , using equation (2).

Find the mass after merge, m_i , using equation (3) and

screen the merge size: $\alpha_i^j = 0$ if $m_i < 0.5$.

UNTIL $k = 1$

STORE: Clustering scores: $S_j = \max_{1 \leq i \leq n-1} \alpha_i^j$

FEATURE SCREENING: $\widehat{\mathcal{I}}_S = \{j : S_j \geq \alpha_0\}$

Next, we provide intuition on some of the key ingredients of our screening algorithm.

Convex Merging Algorithm. With the goal of checking unimodality for each of the feature coordinates, we consider the following univariate optimization problem:

$$\min_{c_1, \dots, c_n \in R} \sum_{i=1}^n (x_i - c_i)^2 + \lambda \sum_{1 \leq k < l \leq n} |c_k - c_l|. \quad (1)$$

It is based on the observations x_i and corresponds to minimizing the within cluster sum of squares under constraints on the ℓ_1 distance between the cluster centroids c_k . Here λ is a non-negative penalty weight. The convexity of the objective function in (1) has been exploited to develop algorithms for efficiently producing the path of solutions as a function of the penalty weight (Hoefling, 2010; Hocking et al., 2011; Radchenko & Mukherjee, 2014). Clustering algorithms based on fusion penalization of this type have become very popular in large scale clustering (Hocking et al., 2011; Radchenko & Mukherjee, 2014; Zhu et al., 2014; Tan & Witten, 2015; Chi & Lange, 2015) and regression analysis (Bondell & Reich, 2008; Ke et al., 2013; Shen & Huang, 2010; Shen et al., 2012).

The solution of the objective criterion (1) can be found for all values of λ by a simple merge algorithm in $O(n \log n)$ operations. Starting with n observations in n clusters, we sequentially merge the nearest (in terms of the weighted distance as shown in Algorithm 1) adjacent centroids until we are left with just one cluster in the end.

Merge Sizes. For each merge on the path, we can explicitly track (Algorithm 1) the parameter λ , as well as the merge size, which is defined for the i -th merge as

$$\alpha_i = n^{-1} \min\{|\mathcal{C}_{i_1}|, |\mathcal{C}_{i_2}|\}, \quad (2)$$

where $|\mathcal{C}_{i_1}|$ and $|\mathcal{C}_{i_2}|$ are the cardinalities of the two corresponding sub-clusters. The fundamental working principle of our proposed COSCI algorithm rests on the following property of the merge sizes: if x_1, \dots, x_n are indeed generated by a non-informative density, then the sample merges $\{\alpha_i : 1 \leq i \leq n - 1\}$ will be uniformly small for sufficiently large n . This property is formalized in Theorem 1 below. On the other hand, if the underlying distribution contains a moderate amount of cluster information, then the merge sequence will have at least one merge that is *big*. The last fact is illustrated by Theorem 1 in Radchenko & Mukherjee (2014). Based on these properties of the merge sequences, we conduct the following screening procedure.

Screening the Merges. Given a pre-defined threshold α_0 , we flag the feature as potential “signal”, if there exists a merge, say the i^{th} merge, such that

$$\alpha_i > \alpha_0 \quad \text{and} \quad m_i := n^{-1} (|\mathcal{C}_{i_1}| + |\mathcal{C}_{i_2}|) \geq 0.5. \quad (3)$$

The restriction on the *mass after merge*, m_i , ensures that we only identify a merge as big if it results in a significantly large cluster. This protects us from the risk of discovering potential big merges on smaller fragments of the sample, where the nature of these merges can be very fragile due to sampling fluctuations. In Algorithm 1, the after merge size control of equation (3) is easily implemented by just resetting the merge sizes to 0 if the mass after merge is less than 0.5. Under mild regularity conditions, the aforementioned fundamental properties of our proposed COSCI algorithm are established in Section 2.1 and its associated Appendix 6.1. As far as the implementation is concerned, a significant gain in computational time is achievable via a parallel implementation of the top *for* loop in Algorithm 1 that runs across the p features.

2.1 Theoretical Support: Perfect Screening Property

Let \mathcal{I}_S and \mathcal{I}_N be the index sets corresponding to the “signal” and the “noise” features, respectively. Define $p_S = |\mathcal{I}_S|$ and $p_N = |\mathcal{I}_N|$. Given feature j , we write $S_j(\tau)$ for the corresponding largest merge size, computed the same way as S_j in Algorithm 1, but under the restriction that the midpoint between the two merged sub-clusters lies between the 100τ -th and $100(1 - \tau)$ -th sample quantiles. Here τ is an arbitrarily small but positive number.

Theorem 1, stated below, establishes a uniform non-asymptotic bound on the merge sizes that are produced when our procedure is applied to the noise features. The regularity conditions, C1 and C2, are imposed on the family of marginal distributions of the noise features, and are fairly mild. In particular, they are satisfied for location-scale families of unimodal differentiable densities with a finite first moment, as long as the corresponding location and scale parameters are uniformly bounded. The proof of Theorem 1 is provided in Appendix 6.1.

Theorem 1. *Suppose that regularity conditions C1 and C2, stated in Appendix 6.1, are satisfied. For each $\tau > 0$ there exist positive constants c_1, c_2, b and κ , whose choice does not depend on either n or p_N , such that, as long as $p_N \leq \exp(\kappa n)$, inequalities*

$$\max_{j \in \mathcal{I}_N} S_j(\tau) \leq b \frac{\log(p_N \vee n)}{n}$$

hold with (high) probability bounded below by $1 - c_1 p_N^{-c_2}$.

The above theorem provides the theoretical justification for the screening step in our proposed procedure. The result is non-asymptotic, and the proof involves careful analysis of the empirical process associated with the merging algorithm for each feature. Under a mild restriction on the number of features relative to the sample size, the above theorem ensures that the clustering scores of all the noise features are uniformly very close to zero. Thus, if we use any arbitrarily small but prefixed value for the threshold α_0 , we have theoretical guarantees for *perfectly screening out* all the noise coordinates. It is important to have a small value of α_0 to avoid screening out the informative features, which have non-negligible clustering scores S_j . Theorem 1 suggests that $\alpha_0^{\text{OR}} = b \log(p \vee n)/n$ is a reasonable choice. Provided n is sufficiently large, an approach using the above choice of α_0 will not screen out the features identified as multi-cluster features by the *population clustering procedure*, defined in Section 2.2 of Radchenko & Mukherjee (2014). The next result, which is a consequence of Theorem 1 above and Theorem 1 in Radchenko & Mukherjee (2014), formalizes this point. Note that Radchenko & Mukherjee (2014) demonstrate, through simulations and theoretical analysis, that the population procedure generally classifies multi-modal distributions as multi-cluster, provided the corresponding sub-populations are of reasonable size.

Corollary 1. *Suppose that regularity conditions C1 and C2, stated in Appendix 6.1, are*

satisfied. Let the cardinality of the set \mathcal{I}_S be bounded above by a universal constant. Suppose that the population clustering procedure identifies each feature in \mathcal{I}_S as multi-cluster. Then, for all sufficiently small $\tau > 0$ there exist positive constants c_1 , c_2 , b and κ , whose choice does not depend on either n or p , such that

$$P(\{j : S_j(\tau) > \alpha_0^{\text{OR}}\} = \mathcal{I}_S) \geq 1 - c_1 p^{-c_2},$$

as long as $p \leq \exp(\kappa n)$.

We view α_0^{OR} as the *oracle choice* of the threshold. However, it is difficult to evaluate it from the data, primarily because the constant b depends on the marginal densities g_j of the noise features. In the following section we discuss several practical choices for the threshold parameter.

3 Estimation of hyperparameters

The COSCI procedure presented in Algorithm 1 requires only one tuning parameter, α_0 , as an input. The *oracle threshold choice* α_0^{OR} is difficult to estimate from the data, as the marginal distributions of the features are typically unknown. In what follows, we present two approaches for estimating α_0 that are adaptive to the sample size n , in the sense that a larger threshold is chosen for smaller sample sizes.

3.1 Simulation based

We generate data of varying sample sizes from several well-known unimodal distributions and use it to assess at which values of α_0 COSCI will detect no clusters, screen out the corresponding noninformative feature. The eight unimodal distributions considered in Table 8 are meant to represent the spectrum of the noise coordinates that are commonly encountered in real data applications. They include symmetric densities with the support equal to the entire R , densities with heavy tails and those with bounded support.

Table 8 in Appendix 6.7 presents the results of this simulation exercise over 100 repetitions. For example, when the noise coordinate is Gaussian, and the sample size is $n = 500$, COSCI detects clusters in the majority of the 100 repetitions when $\alpha_0 \leq 0.05$. Thus, an

appropriate threshold for this case should at least be greater than 0.05. For larger sample sizes, COSCI detects no clusters with a relatively smaller α_0 . A general theme that emerges from this table is that when the underlying density is non-Gaussian with support over entire R or R^+ , smaller thresholds seem to succeed at screening out the corresponding feature, when compared to the Gaussian case for the same sample size. Similarly to the Gaussian case, densities with bounded support, such as the Beta and the Triangular distribution, require a larger threshold to succeed. Our practical recommendation is to assume an underlying Gaussian noise distribution and use α_0 as the smallest threshold that detects no clusters given the sample size n . Let $\hat{\alpha}_0$ be such a threshold. Then, the selected feature set is $\hat{\mathcal{I}}_S = \{j : S_j \geq \hat{\alpha}_0\}$.

3.2 Data driven

In this section, we use a data driven technique to estimate α_0 . We work under the large-scale multiple testing framework of [Efron \(2007\)](#) and transform the problem of estimating α_0 into a problem of feature selection using the merge sizes $\{S_j\}_1^p$. One can then read off the optimal α_0 from the selected features as $\hat{\alpha}_0 = \min_{j \in \hat{\mathcal{I}}_S} S_j$ where $\hat{\mathcal{I}}_S$ holds the indices of the selected features. Let $\psi_j = 2S_j$ be the test statistic for testing the significance of cluster strength in feature j . Note that ψ_j 's have a mixture density f given by: $f(\psi) = \pi_0 f_0(\psi) + (1 - \pi_0) f_1(\psi)$ where f_0 is the *theoretical null* distribution and π_0 is the null prior probability. The exact distributional form of f_0 is, however, unknown, primarily because we do not know the underlying distribution of the noise coordinates that generate the S_j 's. Nonetheless, [Table 8](#) ascertains that f_0 is right skewed on the support $[0, 1]$, with the mass concentrated around zero for large n . We use the MLE method of [Efron \(2007\)](#) to estimate the empirical null distribution from the observed ψ_j 's as a beta distribution and obtain the estimated fdr

$$T_j = \hat{\pi}_0 \hat{f}_0(\psi_j) / \hat{f}(\psi_j) \tag{4}$$

under the prescribed assumption that $\pi_0 \geq 0.9$, i.e, atleast 90% of the p tests are null and $f_1(\psi) = 0$ on \mathcal{A} where $\mathcal{A} = \{\psi_{(1)} \leq \dots \leq \psi_{([0.9p])}\}$. This scheme works reasonably well in both the simulations and the real data examples that we considered. For estimating the mixture density f we adopt Lindsey's method ([Lindsey, 1974](#); [Efron et al., 1996](#)) that models the histogram bin counts using Poisson regression, treating the bin centers as covariates.

Finally, to select the features we adopt the two-stage approach to signal screening recently introduced in [Cai & Sun \(2016\)](#), the details of which are relegated to Appendix 6.4.

In the empirical analysis that follows, we estimate $\widehat{\mathcal{L}}_S$ and $\widehat{\alpha}_0$ using the method described above.

4 Empirical Analysis

4.1 Simulations

We perform several simulation experiments to gauge the feature screening performance of COSCI under two scenarios: (i) $p < n$ and (ii) $p > n$. For scenario (i), we implement two experiments and use the following four competing approaches of feature screening in clustering to compare the performance of our proposed method:

1. Sparse K-Means clustering (SpKM) and Hierarchical clustering (SpHC) ([Witten & Tibshirani, 2012](#)) - we use the R-package `sparcl`.
2. Sparse Alternate Sum (SAS) clustering ([Arias-Castro & Pu, 2016](#)) - we use the R codes available at the author's site (see: https://github.com/victorpu/SAS_Hill_Climb).
3. Important Features PCA (IF-PCA)([Jin & Wang, 2014](#)) - we use the MATLAB codes available at the author's site¹.
4. Excess Mass method (Ex. Mass)([Chan & Hall, 2012](#)) for which unfortunately a software implementation of this method is not available in the public domain. Noting that the excess mass test and the dip test are equivalent in an univariate setting ([Cheng & Hall, 1998](#)), we implement a version of this method for coordinate-wise feature screening using Hartigan's Dip test [([Hartigan & Hartigan, 1985](#)),([Hartigan, 1987](#))]. For feature selection, we select those features for which the multiplicity adjusted ([Benjamini & Hochberg, 1995](#)) p-values from this test are at most 0.05.

For each of the above methods, we are only interested in their feature selection capabilities and not on their clustering performance. For simulation Experiment I, we consider features

¹see: <http://www.stat.cmu.edu/~jiashun/Research/software/HCclustering/>

Table 1: False Negatives and False Positive rates for Simulation Experiment I. Here, $\mathcal{I}_S = \{1, 2, 3, 4, 5\}$, $p = 50$. The numbers in parenthesis are standard errors over 50 repetitions.

		n = 200		n = 1000		n = 2500	
		Avg FN	Avg FP	Avg FN	Avg FP	Avg FN	Avg FP
COSCI with α_0 fixed	0.05	0.06 (0.03)	42.38 (0.22)	0.10 (0.04)	21.26 (0.53)	0.14 (0.06)	6.08 (0.33)
	0.08	0.22 (0.06)	32.88 (0.35)	0.24 (0.06)	10.24 (0.41)	0.34 (0.08)	2.22 (0.23)
	0.1	0.34 (0.07)	26.96 (0.43)	0.34 (0.07)	7.14 (0.33)	0.40 (0.08)	1.20 (0.17)
	0.12	0.52 (0.08)	22.12 (0.41)	0.50 (0.1)	5.16 (0.27)	0.48 (0.09)	0.82 (0.11)
	0.15	0.74 (0.1)	16.16 (0.48)	0.76 (0.1)	3.28 (0.19)	0.64 (0.09)	0.50 (0.1)
	0.2	1.12 (0.1)	9.36 (0.4)	1.04 (0.1)	1.68 (0.15)	0.92 (0.09)	0.30 (0.08)
Data driven		1.8 (0.06)	0.54 (0.13)	0.88 (0.1)	2.14 (0.17)	0.36 (0.08)	1.28 (0.1)
Other methods	SpKM	2.96 (0.24)	16.04 (2.28)	3.26 (0.26)	13.28 (2.27)	3.9 (0.41)	7.00 (4.19)
	SpHC	3.34 (0.21)	16.86 (1.15)	2.08 (0.19)	22.54 (0.77)	1.6 (0.40)	24.5 (2.02)
	SAS	1.46 (0.14)	19.66 (1.15)	1.70 (0.18)	19.52 (1.29)	1.86 (0.2)	17.04 (1.25)
	Ex. Mass	2.3 (0.09)	0.00 (0.00)	2.00 (0.00)	0.00 (0.00)	2.00 (0.00)	0.00 (0.00)
	IF-PCA	0.32 (0.07)	17.64 (0.93)	0.10 (0.04)	18.08 (0.86)	0.10 (0.04)	17.24 (0.99)

from a wide range of parametric distributions including correlated features and consider three different sample sizes from low to high. Simulation experiment I represents scenario (i); we fix $p = 50$ and consider a design matrix $X_{n \times 50}$ with $p_S = 5$ and $p_N = 45$. The p_N noise coordinates are taken to be iid standard Gaussian while the p_S signal coordinates are chosen as follows:

1. $X_1 \sim 0.5 \text{Beta}(4, 6) + 0.5 \text{Beta}(7, 3)$
2. $X_2 \sim 0.5 \text{Lognormal}(0.2, 0.35) + 0.5 \text{Lognormal}(4, 0.5)$
3. $X_3 \sim 0.5 \text{Double Exponential}(3, 1.5) + 0.5 \text{Double Exponential}(5, 1.5)$, and,
4. $(X_4, X_5) \sim (1/4) \sum_{i=1}^4 N(\mu_i, \Sigma_i)$ where

$$\mu_1 = (0, 0), \mu_2 = (0, -4), \mu_3 = (4, 0), \mu_4 = \mu_3 + \mu_2$$

$$\Sigma_1 = \Sigma_4 = \begin{pmatrix} 1 & -0.85 \\ -0.85 & 1 \end{pmatrix}, \Sigma_2 = \Sigma_3 = \begin{pmatrix} 1 & 0.85 \\ 0.85 & 1 \end{pmatrix}$$

In this setting, the signal coordinates are all bi-modal and with the exception of X_1, X_3 , the separation between the adjacent medians is fairly large. For Experiment II, we fix $p = 100$ and consider a design matrix $X_{n \times 100}$ with $p_S = 6$ and $p_N = 94$. We let half of the p_N noise coordinates to be iid standard Gaussian and the other half to be iid t random variables with 5 degrees of freedom. The p_S signal coordinates are chosen as follows:

1. $(X_1, \dots, X_5) \sim$ as experiment 1
2. $X_6 \sim 0.3 N(-2.5,1) + 0.3 N(0,1) + 0.4 N(2.5,1)$ which is a non-symmetric, tri-modal density.

For each of the setups described above, columns of the data matrix X are simulated for $n = 200, 1000$ and 2500 . We analyze two variants of COSCI: (i) COSCI with α_0 fixed over a grid of six values, $\{0.05, 0.08, 0.1, 0.12, 0.15, 0.2\}$ and, (ii) COSCI with α_0 estimated in a data driven fashion as discussed in Section 3.2. For each method we calculated two statistics averaged over 50 repetitions: False Negative (FN) - the number of signal features incorrectly identified as noise; False Positive (FP) - the number of noise features incorrectly identified as signal. From Table 1, it is evident that SpKM fails to detect atleast 3 out of

Table 2: False Negatives and False Positive rates for Simulation Experiment II. Here, $\mathcal{I}_S = \{1, 2, 3, 4, 5, 6\}$, $p = 100$. The numbers in parenthesis are standard errors over 50 repetitions.

		n = 200		n = 1000		n = 2500	
		Avg FN	Avg FP	Avg FN	Avg FP	Avg FN	Avg FP
COSCI with α_0 fixed	0.05	0.06 (0.03)	84.76 (0.41)	0.1 (0.04)	34.62 (0.71)	0.14 (0.06)	8.2 (0.44)
	0.08	0.22 (0.06)	61.9 (0.57)	0.38 (0.08)	15.18 (0.54)	0.58 (0.11)	2.64 (0.25)
	0.1	0.38 (0.08)	49.5 (0.64)	0.52 (0.09)	10.3 (0.4)	0.76 (0.12)	1.38 (0.18)
	0.12	0.6 (0.09)	39.32 (0.62)	0.72 (0.12)	7.34 (0.3)	0.96 (0.11)	0.96 (0.13)
	0.15	0.88 (0.1)	28.16 (0.62)	1.06 (0.13)	4.86 (0.26)	1.36 (0.12)	0.58 (0.11)
	0.2	1.4 (0.11)	15.9 (0.52)	1.74 (0.12)	2.46 (0.19)	1.86 (0.1)	0.34 (0.09)
Data driven		1.66 (0.08)	2.04 (0.28)	0.86 (0.11)	6.98 (0.24)	0.18 (0.06)	7.04 (0.27)
Other methods	SpKM	4.36 (0.25)	29.04 (3.23)	5.02 (0.26)	18.42 (3.93)	5.5 (0.5)	14.00 (8.56)
	SpHC	3.52 (0.27)	38.6 (3.05)	1.54 (0.23)	61.9 (3.18)	-	-
	SAS	1.14 (0.15)	58.48 (1.91)	2.1 (0.28)	41.66 (2.95)	1.82 (0.27)	43.9 (2.95)
	Ex. Mass	2.36 (0.10)	0.00 (0.00)	2.00 (0.00)	0.00 (0.00)	2.00 (0.00)	0.00 (0.00)
	IF-PCA	1.96 (0.15)	18.46 (2.24)	0.3 (0.06)	38.84 (0.61)	0.14 (0.05)	42.36 (0.23)

the 5 signal features across the three sample sizes, while SpHC and SAS have relatively better FN performance. The SpHC algorithm faced scalability issues (marked by dash in the table) for 2500 sample sizes. IF-PCA, on the other hand, correctly identifies the 5 signal features. All of these four methods have high false positives. Variations in sample sizes do not seem to affect their performance in any significant manner. Ex. Mass consistently fails to identify multi-modality in X_1 and X_3 but has the best false positive performance across all the methods. This is not unexpected given that the noise features considered are uni-modal. For α_0 small, COSCI identifies the 5 signal features (low FN rate) but also

incorrectly includes many noise features as signals (high FP rate). As expected, this trend transitions into a high FN rate and low FP rate for larger α_0 's. This is where the data driven approach to choose α_0 is seen to be beneficial. For moderately large n , COSCI, coupled with the data driven approach, returns a FN rate comparable to IF-PCA but with a significantly smaller FP rate. The results in Table 2 reveal a similar picture. When both FN and FP rates are taken into consideration, COSCI delivers the best performance amongst all the competing methods for moderately large n . Even when $n = 200$, COSCI returns a FN rate which is only slightly higher than IF-PCA and SAS but enjoys a far better FP rate.

The next two simulation experiments III and IV exemplify scenario (ii) where $p > n$. We consider noise features which include non-symmetric distributions like Exponential with rate parameter 1 and heavy-tailed distributions like standard Cauchy. This presents an interesting setting especially for methods like IF-PCA that rely on statistical comparison with a fixed parametric distribution to determine feature importance for clustering. In experiment III, we have $p = 5000$ and $p_S = 7$ with

1. $(X_1, \dots, X_6) \sim$ as in Experiment I
2. $X_7 \sim 0.5 N(-1.1,1) + 0.5 N(1.1,1)$.

Note that X_7 is a bi-modal Gaussian mixture but with a relatively small separation between the modes. The p_N noise features consists of approximately 40% iid Exp(1) noise along with 30% iid standard Gaussian and 30% iid t_5 noise. For Experiment IV, we consider $p = 25000$ and add two more signal features so that $p_S = 9$ with

1. $(X_1, \dots, X_7) \sim$ as in Experiment III
2. $X_8 \sim 0.3 \text{ Double Exponential}(-3,1) + 0.35 \text{ Double Exponential}(0,1) + 0.35 \text{ Double Exponential}(3,1)$.
3. $X_9 \sim 0.3 \text{ Beta}(8,2) + 0.35 \text{ Beta}(5,5) + 0.35 \text{ Beta}(2,8)$

Here X_8, X_9 , once again, represent features with a relatively small separation between the modes and, thus, are particularly difficult examples for modality detection. The p_N noise features here include approximately 28% iid standard Cauchy noise along with 24% iid standard Gaussian, 24% iid t_5 and 24% iid Exp(1) noises. We keep all the other design parameters of Experiment IV identical to Experiment III. However, we do not include the

performance of SpKM, SpHC and SAS in our analysis of Experiment IV as these algorithms are computationally very demanding and often exhibited convergence issues in this regime. From Tables 3 and 4, a drop in the FN performance of both IF-PCA and Ex. Mass

Table 3: False Negatives and False Positive rates for Simulation Experiment III. Here, $\mathcal{I}_S = \{1, 2, 3, 4, 5, 6, 7\}$, $p = 5000$. The numbers in parenthesis are standard errors over 50 repetitions.

		n = 200		n = 1000		n = 2500	
		Avg FN	Avg FP	Avg FN	Avg FP	Avg FN	Avg FP
COSCI with α_0 fixed	0.05	0.12 (0.05)	4341.6 (3.13)	0.82 (0.08)	1,355.3 (3.84)	1.06 (0.07)	274.62 (2.56)
	0.08	0.48 (0.08)	2979.62 (5.06)	1.26 (0.09)	548.8 (3.11)	1.58 (0.11)	82.86 (1.30)
	0.1	0.84 (0.11)	2279.44 (4.37)	1.44 (0.1)	349.68 (2.04)	1.76 (0.12)	47.5 (1.08)
	0.12	1.22 (0.12)	1764.22 (5.09)	1.68 (0.12)	242.7 (1.75)	1.96 (0.11)	30.8 (0.83)
	0.15	1.56 (0.13)	1215.96 (4.86)	2.04 (0.13)	151.74 (1.21)	2.36 (0.12)	17.64 (0.62)
	0.2	2.22 (0.12)	636.62 (3.68)	2.72 (0.13)	69.58 (0.96)	2.86 (0.1)	7.74 (0.44)
	Data driven	2.68 (0.12)	297.14 (6.50)	1.32 (0.1)	498.76 (2.86)	0.92 (0.07)	516.28 (4.19)
Other methods	Ex. Mass	4.86 (0.14)	0.00 (0.00)	4.00 (0.00)	0.00 (0.00)	4.00 (0.00)	0.00 (0.00)
	IF-PCA	5.68 (0.09)	1802.4 (4.29)	6.00 (0.00)	1943.6 (1.86)	6.00 (0.00)	1970.00 (0.88)

Table 4: False Negatives and False Positive rates for Simulation Experiment IV. Here, $\mathcal{I}_S = \{1, 2, 3, 4, 5, 6, 7, 8, 9\}$, $p = 25000$. The numbers in parenthesis are standard errors over 10 repetitions.

		n = 200		n = 1000		n = 2500	
		Avg FN	Avg FP	Avg FN	Avg FP	Avg FN	Avg FP
COSCI with α_0 fixed	0.05	0.12 (0.05)	18587.2 (8.03)	0.6 (0.22)	5310.00 (22.81)	1.00 (0.1)	1101.67 (11.5)
	0.08	0.48 (0.08)	12176.00 (10.6)	1.30 (0.3)	2170.00 (11.71)	1.47 (0.192)	339.2 (4.82)
	0.1	0.84 (0.11)	9221.48 (10.01)	1.50 (0.27)	1397.5 (9.96)	1.6 (0.19)	196 (2.68)
	0.12	1.22 (0.12)	7088.34 (9.18)	1.70 (0.26)	976.5 (8.16)	1.73 (0.18)	126 (2.99)
	0.15	1.60 (0.13)	4862.02 (8.61)	2.10 (0.28)	616.40 (7.22)	2.00 (0.22)	72.87 (2.41)
	0.2	2.42 (0.12)	2537.76 (6.92)	2.60 (0.27)	279.5 (3.27)	2.8 (0.22)	29.07 (1.65)
	Data driven	2.84 (0.14)	1687.34 (17.77)	1.40 (0.30)	1928.3 (18.72)	1.00 (0.1)	1324.8 (19.27)
Other methods	Ex. Mass	7.16 (0.13)	0.00 (0.00)	6.00 (0.00)	0.00 (0.00)	5.2 (0.11)	0.00 (0.00)
	IF-PCA	9.00 (0.00)	4061.2 (17.71)	9.00 (0.00)	5286.5 (17.64)	9.00 (0.00)	5563.3 (12.97)

is conspicuous. For IF-PCA, the non-Gaussian noises are identified as signals which are ultimately selected in favor of the true signals under the HC functional. Ex. Mass on the other hand continues to conclude some of the difficult multi-modal signals like X_1, X_3, X_7, X_8 and X_9 as unimodal. COSCI, with the data driven approach, once again returns the best performance across all the different sample size regimes considered in these two experiments.

4.2 Real Data Examples

We test the performance of COSCI on a number of real data examples. In all these datasets, the number of clusters / subpopulations is known apriori. However, unlike the simulation study, we do not know the ‘true’ feature set for these datasets and thus an estimate of screening performance based on False Negatives or False Positives is impossible. Instead, we use the following scheme to gauge the performance of COSCI. On each of the datasets considered in this section, we overlay COSCI with k -means (KM), Sparse k -means (SpKM) and IF-PCA. In other words, we allow COSCI to screen and select the best features and thereafter, we run classical k -means, Sparse k -means and IF-PCA on the selected features. While using IF-PCA on the COSCI screened features, we only use the clustering component of IF-PCA and not its feature selection step. The classification error rates (CER) so obtained from the above 3 schemes are then compared to the CER of the competing methods- k -means, Sparse k -means and IF-PCA, all without any COSCI screening. For k -means and IF-PCA, we report the average CER over 30 independent replications and the associated standard error whenever they are bigger than 0.0005. Next, we describe in details the application of the aforementioned methods on three real datasets. In Appendix 6.5 the classification results on eleven other datasets are also demonstrated.

Multi-tissue Data - This is a microarray data on different mammalian tissue types. The data was produced by [Su et al. \(2002\)](#) and it holds gene expression from human and mouse samples across a diverse array of tissues, organs and cell lines. There are 102 samples (n) and 5565 genes (p) in this data. The tissue types have 4 categories that are known and the goal is to identify the sub-populations that correspond to the 4 tissue types. This data can be publicly sourced from the R-package FABIA ([Hochreiter et al., 2010](#)). In figure 2, we plot the distribution of ψ_j (left) alongwith the rank ordering of the 5565 features with respect to the scores S_j (right). Using the data driven selection procedure, COSCI selects the top 4 features and returns an estimate of α_0 almost close to 0.4 which agrees well with the threshold choice prescribed in Table 8 for sample size 100 and Gaussian noise coordinates. CERs for the aforementioned classification methods are reported in Table 5.

Cardio Data - This data has 63 subjects (n) of which 19 are cardiovascular patients and the rest are healthy controls. The genetic expression of each subject has been recorded for

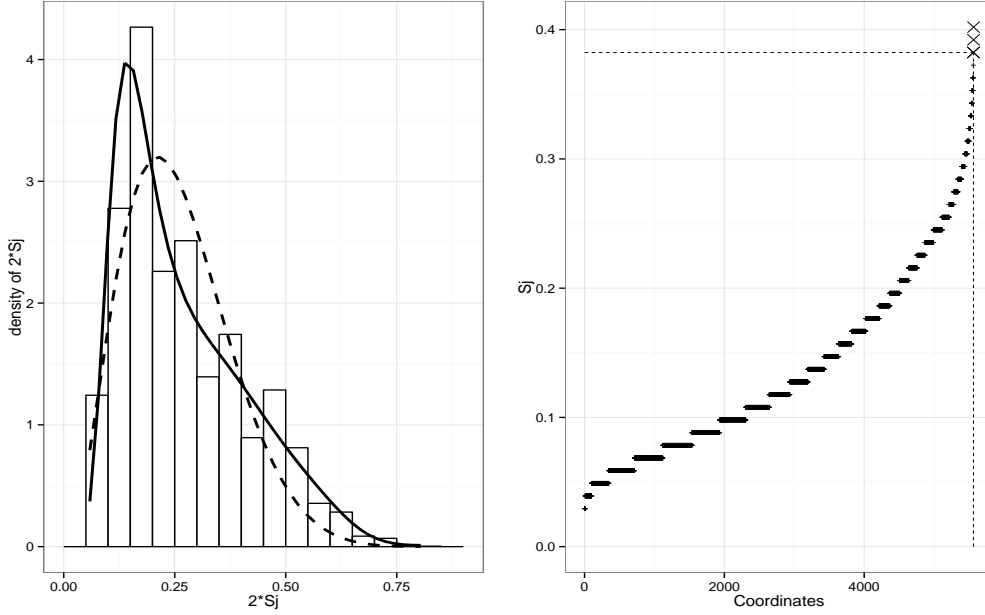


Figure 2: MULTI-TISSUE DATA. Left: $\hat{\pi}_0 \hat{f}_0(\psi_j)$ in black dashed line and $\hat{f}(\psi_j)$ in black solid line for $j = 1, 2, \dots, 5565$. Right: Distribution of S_j . The 4 selected features are marked as \times . The dashed horizontal line is $\hat{\alpha}_0 = 0.382$.

20,426 genes (p). The goal is to classify the subjects as healthy or cardiovascular based on expression levels of the p genes. The dataset is publicly available on Brad Efron’s webpage.

In figure 3 (Appendix 6.6), we plot the distribution of ψ_j (left) along with the rank ordering of the 20,426 features with respect to the scores S_j (right). Using the data driven selection procedure, COSCI selects the top 33 features and results in an estimate of α_0 equal to 0.428. Due to the small sample size of this data, the data driven procedure returns an unrealistic estimate of null proportion $\hat{\pi}_0 = 0.99$ when the empirical null distribution is estimated on $\mathcal{A} = \{\psi_{(1)} \leq \dots \leq \psi_{([0.9p])}\}$. We comment more on this observation after introducing the results in Table 5.

RNASeq Data - The RNASeq data discussed in Section 1 is an example where both n and p are large. For such large values of n , one would expect an asymptotic regime to kick in and hope to see the distribution of ψ_j ’s concentrated around a small value. In figure 4 (Appendix 6.6) (left), we see that approximately 70% of the coordinates have $\psi_j \leq 0.1$. Moreover, the distribution of S_j (figure 4 right) has an explicit ‘elbow’ at 0.1, suggesting that we could take the cut-off on α_0 to be 0.1 and select those features with $S_j \geq 0.1$. This is indeed one of the ways that we can approach the problem given this data and that would

have left us with ~ 2800 features. We, however, continue with the data driven approach but take $\mathcal{A} = \{\psi_{(1)} \leq \dots \leq \psi_{([0.7p])}\}$. This leads to an estimated null proportion $\hat{\pi}_0 = 0.70$ with the top 2304 features as the selected ones. Estimated $\hat{\alpha}_0$ is 0.188 which (i) is not far from the ‘elbow’ in the distribution of S_j and (ii) once again agrees well with the theoretical choice prescribed under Gaussian noises in Table 8.

Table 5: This table has 3 parts. In the first part of the table, we provide some preliminary information on the 3 datasets. The second part of the table has CER for the 3 competing methods. For IF-PCA, we also report the number of selected features after the ‘/’ symbol. In the last part of the table, CER for COSCI + ‘clustering method’ is reported alongwith the number of selected features. The numbers in parenthesis are standard errors over 30 repetitions of k -means and IF-PCA. The standard errors are only reported when they exceed 0.0005. The SAS algorithm faced scalability issues (marked by dash) for RNASeq data

		Multi-tissue	Cardio	RNASeq
Prelim. info.	n	102	63	2730
	p	5565	20426	8716
	# clusters	4	2	19
Competing methods	SpKM	0.698	0.492	0.157
	KM	0.721 (0.002)	0.493	0.157
	SAS	0.554 / 1307	0.492 / 1071	-
	Ex. Mass	no selection	no selection	0.157 / 6814
	IF-PCA	no selection	0.486 / 523	0.213 (0.002) / 4358
COSCI +	SpKM	0.396 / 4	0.505 / 33	0.152 / 2304
	KM	0.397 / 4	0.505 / 33	0.153 / 2304
	IF-PCA	0.381 / 4	0.505 / 33	0.156 / 2304

We make several comments on the CER’s reported in Table 5. The general theme of those results is compelling. These examples suggest that feature screening by COSCI can potentially lead to improvements in clustering error rates even when the underlying clustering algorithm is vanilla k -means. On the Multi-tissue data, IF-PCA and Ex. Mass fail to select any feature whereas the 4 COSCI screened features overlaid with IF-PCA clustering clearly demonstrates substantial improvement over the competing error rates. A similar observation follows when COSCI is overlaid with Sparse k -means and k -means. On the RNASeq data, k -means performs well but in this example too, COSCI screening leads to an overall improvement in the error rate with much fewer features. On the Cardio data, performance enhancement is not observed primarily due to the small sample size of this data. For such low values of n , the added dispersion in the empirical null often

masks relatively weaker signals from being identified. In these cases, the empirical null distribution may be estimated on a slightly smaller set $\mathcal{A} = \{\psi_{(1)} \leq \dots \leq \psi_{([0.85p])}\}$ to improve clustering accuracy at the expense of a few more features. For example, on the Cardio data with \mathcal{A} as prescribed above, COSCI selects only 129 features but returns a comparable CER of 0.486 using k -means.

4.3 Beyond Marginal Screening: 2-way interactions

In this section we consider an extension of COSCI that can successfully identify pairs of features that hold cluster information jointly but are un-informative marginally. Screening procedures like Excess Mass that rely on marginal screening can easily miss these interacting features and label them as noise.

As alluded to in Section 2, we expect that these pairs of features will reveal their inherent cluster strength through a suitable linear combination of the form $X^{i,j}u$ where $X_{n \times 2}^{i,j}$ is the feature pair using the (i, j) feature in X and $u \in R^2$ with $\|u\|_2 = 1$. To determine the optimal u for each feature pair (i, j) , we use a grid search in R^2 as follows.

1. Generate a uniform grid of m points u_k on the unit circle in R^2 .
2. For the feature pair (i, j) , define $Y_{n \times m} = \{X^{i,j}u_k : 1 \leq k \leq m\}$ and use Algorithm 1 to get $S_{(i,j)}(u_1), \dots, S_{(i,j)}(u_m)$ for the m features in Y .
3. Obtain the feature score for the pair (i, j) as $S_{(i,j)} = \max_{1 \leq k \leq m} S_{(i,j)}(u_k)$ and the optimal u as $u_{(i,j)}^* = \operatorname{argmax}_{1 \leq k \leq m} S_{(i,j)}(u_k)$.

We repeat this procedure for all the $\binom{p}{2}$ feature pairs and choose

$$\widehat{\mathcal{I}}_S = \operatorname{unique}\left(\{i : S_i \geq \alpha_0\} \cup \{(i, j) : S_{(i,j)} \geq \alpha_0\}\right)$$

Often a component of $u_{(i,j)}^*$ will be small indicating that one of the contributing features in the pair (i, j) dominates the other in terms of cluster strength. In these scenarios, we may run into the problem of including a lot of redundant pairs in $\widehat{\mathcal{I}}_S$ due to the strong effect of only one of the features. Such issues are easily resolved by using a naive thresholding rule

on $u_{(i,j)}^*$ to select the features and modifying $\widehat{\mathcal{I}}_S$ accordingly:

$$\widehat{\mathcal{I}}_S^{\text{thr}} = \begin{cases} \{(i, j) : S_{(i,j)} \geq \alpha_0 \text{ and } \max_{l=1,2} |u_{(i,j)}^*(l)| < 0.95\} \\ \{i : S_{(i,j)} \geq \alpha_0 \text{ and } |u_{(i,j)}^*(1)| \geq 0.95\} \\ \{j : S_{(i,j)} \geq \alpha_0 \text{ and } |u_{(i,j)}^*(2)| \geq 0.95\}, \end{cases}$$

$$\widehat{\mathcal{I}}_S^{\text{mod}} = \text{unique}\left(\{i : S_i \geq \alpha_0\} \cup \widehat{\mathcal{I}}_S^{\text{thr}}\right).$$

To demonstrate the effectiveness of this approach, we consider a simple simulation setting (Experiment V) with $m = 20$, $p_S = 4$, $p_N = 21$ and $n = 2000$. We let the p_N noise features be iid Standard Normal. For the signal coordinates, we take

1. $(X_1, X_2) \sim (1/2) \sum_{i=1}^2 N(\mu_i, \Sigma)$
2. $X_3 \sim 0.5 \text{Beta}(4, 6) + 0.5 \text{Beta}(7, 3)$
3. $X_4 \sim 0.5 \text{Log Normal}(0.2, 0.35) + 0.5 \text{Log Normal}(4, 0.5)$, where

$$\mu_1 = (0.9, -0.9), \mu_2 = -\mu_1, \text{ and } \Sigma = \begin{pmatrix} 1 & 0.9 \\ 0.9 & 1 \end{pmatrix}$$

In this setting features X_3 and X_4 are bi-modal but (X_1, X_2) are only jointly bi-modal. Note that the effective dimensionality of the data in this example is $p_S + p_N + m \binom{p_S + p_N}{2} = 6025$. In table 6, we report the *False Positive* and *False Negative* proportions produced by applying the aforementioned extension of our proposed COSCI algorithm. It successfully identifies all the signal coordinates. As expected, higher values of the threshold parameter improve the FP rate, and the benefit of using the data driven approach to select the features is evident. Once again, the prescribed theoretical choice (Table 8), for the Gaussian noises (with $n = 2000$) agrees with these results.

5 Discussion

We propose COSCI, a novel feature screening method for large scale cluster analysis problems that are characterized by both large sample sizes and high dimensionality of the observations. COSCI efficiently ranks the candidate features in a non-parametric fashion

Table 6: False Negatives and False Positive rates for Simulation Experiment V. Here, $\mathcal{I}_S = \{1, 2, 3, 4\}$, $p = 25$. The numbers in parenthesis are standard errors over 10 repetitions.

n = 2000 / p = 25			
		Avg FN	Avg FP
	0.05	0.00 (0.00)	21.00 (0.00)
COSCI	0.08	0.00 (0.00)	21.00 (0.00)
with	0.1	0.00 (0.00)	20.9 (0.1)
α_0	0.12	0.00 (0.00)	20.3 (0.26)
fixed	0.15	0.00 (0.00)	18.8 (0.39)
	0.2	0.00 (0.00)	13.7 (0.68)
	0.25	0.00 (0.00)	3.8 (0.78)
Data driven		0.00 (0.00)	3.1 (0.23)

and, under mild regularity conditions, is robust to the distributional form of the true noise coordinates. We establish theoretical results supporting ideal feature screening properties of our proposed procedure and provide a data driven approach for selecting the screening threshold parameter. Extensive simulation experiments and real data studies demonstrate encouraging performance of our proposed approach.

An interesting topic for future research is extending our marginal screening method by means of utilizing multivariate objective criteria, which are more potent in detecting multivariate cluster information among marginally unimodal features. Preliminary analysis of the corresponding ℓ_2 fusion penalty based criterion, which, unlike the ℓ_1 based approach used in this paper, is non-separable across dimensions, suggests that this criterion can provide a way to move beyond marginal screening.

Acknowledgement

The authors thank Sara Garcia and Gregory Giecold for sharing the RNASeq data and ECLAIR source codes with them. Mukherjee’s research was partially supported by the Zumberge individual award from the University of Southern Californias James H. Zumberge faculty research and innovation fund.

Supplementary material

The R code and the data sets used in this paper can be downloaded from <http://github.com/trambakbanerjee/COSCI>.

6 Appendix

6.1 Regularity Conditions and Proofs

Given feature j , an interval (L, R) and a point $a \in (L, R)$, we define the corresponding population criterion function as $G_{L,R}^j(a) = \mu_{a,R}^j - \mu_{L,a}^j$, where $\mu_{l,r}^j$ is the conditional mean on (l, r) under the population distribution of the j -th feature. We use the term population cluster to refer to all intervals that appear along the path of the corresponding univariate population splitting procedure, as defined in [Radchenko & Mukherjee \(2014\)](#).

We now formally state the regularity conditions needed in [Theorem 1](#). We write g_j for the marginal density of the j -th feature, X_j , and let q_j denote the corresponding quantile function.

There exist positive universal constants C_τ and c_τ , which depend only on τ , and a positive universal C , such that for all $j \in \mathcal{I}_N$ and $\tau \in (0, 1)$:

C1 Densities g_j are differentiable and unimodal. Also,

$$\max_{j \in \mathcal{I}_N} E|X_j| < C \quad (5)$$

$$\max_{j \in \mathcal{I}_N} \|g_j\|_\infty + \|g'_j\|_\infty < C \quad (6)$$

$$\max_{j \in \mathcal{I}_N} |q_j(\tau)| + |q_j(1 - \tau)| < C_\tau \quad (7)$$

$$\min_{j \in \mathcal{I}_N} g_j(q_j(\tau)) \wedge g_j(q_j(1 - \tau)) > c_\tau. \quad (8)$$

C2 For each population cluster (L, R) of the j -th feature, satisfying inequality $\int_L^R g_j(x) dx \geq 0.49$, and each $t \in \{L, R\} \cap \arg \max G_{L,R}^j \cap [q_j(\tau), q_j(1 - \tau)]$, we have $|G_{L,R}^{j'}(t)| > c_\tau$.

Condition C1 ensures that we have uniform control over the noise densities. Condition C2 is an appropriate adaptation of a standard regularity condition in M-estimation. As we mentioned earlier, C1 and C2 are satisfied for location-scale families of unimodal differ-

entiable densities with a finite first moment, as long as the corresponding parameters are uniformly bounded.

6.2 Proof of Theorem 1 and Corollary 1

We will use “ \lesssim ” to mean that inequality “ \leq ” holds when the right hand side is multiplied by a positive constant, which is chosen independently from the parameters p , n , j and c_3 (note that the constant is allowed to depend on τ and ϵ_1). To simplify the exposition, we will write p for p_N , and have index j always correspond to the (noise) coordinates in \mathcal{I}_N .

Let L_j and R_j denote the smallest and the largest value, respectively, of the (univariate) cluster formed in the j -th coordinate after the merge corresponding to $S_j(\tau)$. For the same merge, let a_j be the midpoint between the closest representatives of the two sub-clusters. We define the empirical criterion functions as $\widehat{G}_{L,R}^j(a) = \widehat{\mu}_{a,R}^j - \widehat{\mu}_{L,a}^j$, where $\widehat{\mu}_{l,r}$ denotes the average of the observations on the j -th feature that fall in $[l, r]$. We need the following lemma, which is proved in Appendix 6.3.

Lemma 1. *For every positive ϵ_1 and τ , there exist positive constants c_0 , c_3 , c_4 , c_5 and κ , such that, as long as $p \leq \exp(\kappa n)$, the following inequalities simultaneously hold for all j with probability bounded below by $1 - c_4 p^{-c_5}$:*

$$\begin{aligned} & \left| \left(\widehat{G}_{L_j, R_j}^j(R_j) - \widehat{G}_{L_j, R_j}^j(a_j) \right) - \left(G_{L_j, R_j}^j(R_j) - G_{L_j, R_j}^j(a_j) \right) \right| \\ & \leq \epsilon_1(R_j - a_j) + c_3 \frac{\log(p \vee n)}{n}, \end{aligned} \tag{9}$$

$$\begin{aligned} & \left| \left(\widehat{G}_{L_j, R_j}^j(L_j) - \widehat{G}_{L_j, R_j}^j(a_j) \right) - \left(G_{L_j, R_j}^j(L_j) - G_{L_j, R_j}^j(a_j) \right) \right| \\ & \leq \epsilon_1(a_j - L_j) + c_3 \frac{\log(p \vee n)}{n} \end{aligned} \tag{10}$$

$$\left| P_n^j(R_j - a_j) - P^j(R_j - a_j) \right| \leq \epsilon_1(R_j - a_j) + c_3 \frac{\log(p \vee n)}{n}, \tag{11}$$

$$\left| P_n^j(a_j - L_j) - P^j(a_j - L_j) \right| \leq \epsilon_1(a_j - L_j) + c_3 \frac{\log(p \vee n)}{n} \tag{12}$$

$$\begin{aligned} & [G_{L_j, R_j}^j(L_j) - G_{L_j, R_j}^j(a_j)] \vee [G_{L_j, R_j}^j(R_j) - G_{L_j, R_j}^j(a_j)] \\ & \geq c_0(R_j - a_j) \wedge (a_j - L_j). \end{aligned} \tag{13}$$

For the remainder of the proof we restrict our attention to the set on which inequalities (9)-(13) are valid. It follows directly from Proposition 2 in Radchenko & Mukherjee (2014) that $a_j \in \arg \max \widehat{G}_{L_j, R_j}^j$. Taking $\epsilon_1 = c_0/2$ in Lemma 1, we derive

$$\begin{aligned} 0 &\geq [\widehat{G}_{L_j, R_j}^j(L) - \widehat{G}_{L_j, R_j}^j(a_j)] \vee [\widehat{G}_{L_j, R_j}^j(R_j) - \widehat{G}_{L_j, R_j}^j(a_j)] \\ &\geq c_0(R_j - a_j) \wedge (a_j - L_j) - \epsilon_1(R_j - a_j) \wedge (a_j - L_j) + c_3 \frac{\log(p \vee n)}{n} \\ &\geq (c_0/2)(R_j - a_j) \wedge (a_j - L_j) - c_3 \frac{\log(p \vee n)}{n} \end{aligned}$$

Hence, for all j , we have

$$(R_j - a_j) \wedge (a_j - L_j) \leq 2c_0^{-1}c_3 \frac{\log(p \vee n)}{n}.$$

Because the densities are uniformly bounded, the left-hand side can be replaced by $P^j(R_j - a_j) \wedge P^j(a_j - L_j)$ at the cost of an additional universal multiplicative factor on the right-hand side. To complete the proof, it is only left to replace each P^j with the corresponding empirical probability, P_n^j . This replacement is justified (again, at the cost of an additional universal multiplicative factor) by applying inequalities (11) and (12).

6.3 Proof of Lemma 1

We will focus on inequality (9) and, for concreteness, suppose that $a_j \in [(L_j + R_j)/2, R_j]$. The rest of the cases can be handled using analogous arguments.

Applying Theorem 2.14.9 in Van der Vaart & Wellner (1996), together with the union bound, we note that for each positive ϵ we have

$$P(\max_j \sup_{l < r} |P_{nj}(l, r) - P_j(l, r)| > \epsilon) \leq a_1 \exp(-a_2 n - a_2 \log n - a_3 \log p),$$

for some positive constants a_l that only depend on ϵ . Because of the assumption on the magnitude of p , the right hand side in the above display can be bounded by $a_1 p^{-a_4}$. Thus, taking into account condition (7), as well as the definition of a_j , we can conclude that, with the exception of the corresponding set of small probability, all a_j are uniformly bounded. Moreover, applying Theorem 2.14.9 in Van der Vaart & Wellner (1996) again and taking advantage of conditions (5), (6) and (8), we can deduce that all L_j and R_j are restricted to

a uniformly chosen bounded interval, on which all $\|g_j\|_\infty$ and $\|1/g_j\|_\infty$ are bounded.

From now on, we focus on all the triples $L \leq a \leq R$ in the aforementioned bounded interval, for which $\widehat{G}_{L,R}^j(a)$ is well defined. Note that for all such triples, and all j , we have $R - a \lesssim P_j(a, R)$ and $P_j(a, R) \lesssim R - a$. Define $d_{l,r}(x) = (r - x)(r - l)^{-1}1_{\{l < x < r\}}$ and note that

$$\begin{aligned} |\widehat{\mu}_{a,R}^j - \mu_{a,R}^j| &= \left| \frac{P_{nj}d_{a,R}(R - a)}{P_{nj}(a, R)} - \frac{P_jd_{a,R}(R - a)}{P_j(a, R)} \right| \\ &\leq |P_{nj}d_{a,R} - P_jd_{a,R}| \frac{(R - a)}{P_j(a, R)} + |P_{nj}(a, R) - P_j(a, R)| \frac{(R - \widehat{\mu}_{a,R}^j)}{P_j(a, R)} \\ &\lesssim |P_{nj}d_{a,R} - P_jd_{a,R}| + |P_{nj}(a, R) - P_j(a, R)| =: E_1 + E_2. \end{aligned}$$

Let $h_{l,r}(x) = x1_{l < x < r}$. Observe that $|P_{nj}h_{a,R} - P_jh_{a,R}| \lesssim E_2$, and define $D_n = \max_j \sup_{l < r} (|P_{nj}h_{l,r} - P_jh_{l,r}|) + (|P_{nj}(l, r) - P_j(l, r)|)$. It follows that

$$\begin{aligned} &|(\mu_{L,R}^j - \mu_{L,a}^j) - (\widehat{\mu}_{L,R}^j - \widehat{\mu}_{L,a}^j)| \\ &= \left| \frac{P_jh_{L,a}P_j(a, R) + P_jh_{a,R}P_j(L, a)}{P_j(L, R)P_j(L, a)} - \frac{P_{nj}h_{L,a}P_{nj}(a, R) + P_{nj}h_{a,R}P_{nj}(L, a)}{P_{nj}(L, R)P_{nj}(L, a)} \right| \\ &\lesssim E_2 + [(R - a) + E_2] D_n. \end{aligned}$$

Applying Theorem 2.14.9 in [Van der Vaart & Wellner \(1996\)](#), together with the union bound, we note that for each positive ϵ we have

$$P(D_n > \epsilon) \leq a_1 \exp(-a_2 n - a_2 \log n - a_3 \log p),$$

for some positive constants a_l that only depend on ϵ . Because of the assumption on the magnitude of p , the right hand side in the above display can be bounded by $a_1 p^{-a_4}$. Thus, to establish the bound in inequality (9) we only need to verify that it holds for E_1 and E_2 , uniformly over $L \leq a \leq R$ in the aforementioned bounded interval. We will focus on E_2 , as E_1 can be handled with only minor modifications to the argument. We need to show that there exist positive constants c_2 and c_3 and a sequence of random variables M_n , such that

$\mathbb{P}(M_n > c_3) \lesssim p^{-c_2}$ and inequalities

$$|P_{nj}(l, r) - P_j(l, r)| \leq \epsilon_1(r - l) + \frac{\log(p \vee n)}{n} M_n \quad (14)$$

hold for all j and (l, r) contained within the bounded interval. Let M_n^j be the infimum of all those values for which equation (14) holds in the j^{th} coordinate, and define $M_n = \max_j M_n^j$. Recall that we have restricted our attention to a uniformly bounded interval, on which $c_4 := \max_j \|1/g_j\|_\infty$ is positive. Let $\xi_n = \log(p \vee n)/n$, and write $A_{k,n}^j$ for the set of intervals (l, r) that lie inside the aforementioned uniformly bounded interval and satisfy inequalities $[2^{k-1} - 1]\xi_n < P_j(l, r) \leq 2^k \xi_n$. In what follows, constants c_l are positive and can be chosen independently from c_3 , p , n , and j . Observe that

$$\begin{aligned} \mathbb{P}(M_n > c_3) &\leq \sum_j \mathbb{P}(M_n^j > c_3) \\ &\leq \sum_j \sum_{k=1}^{\infty} \mathbb{P}(\exists(l, r) \in A_{k,n}^j \text{ s.t. } |P_{nj}(l, r) - P_j(l, r)| > \epsilon_1(r - l) + c_3 \xi_n) \\ &\leq \sum_j \sum_{k=1}^{\infty} \mathbb{P}\left(\sup_{A_{k,n}^j} |P_{nj}(l, r) - P_j(l, r)| > \xi_n (c_4 \epsilon_1 (2^{k-1} - 1) + c_3)\right). \end{aligned}$$

We will bound each summand in the last expression by applying Theorem 2.14.25 in [Van der Vaart & Wellner \(1996\)](#) with $\mu_n = 2^{k/2} \xi_n \sqrt{n}$ and $\sigma_{\mathcal{F}}^2 = 2^k \xi_n$. Note that μ_n is an upper bound on $\sup_{A_{k,n}^j} \sqrt{n} |P_{nj}(l, r) - P_j(l, r)|$, up to some universal multiplicative factors, as demonstrated in the proof of Lemma 5 in [Radchenko & Mukherjee \(2014\)](#). It follows that

$$\begin{aligned} \mathbb{P}(M_n > c_3) &\leq \sum_j \sum_{k=1}^{\infty} \exp\{-c_5 c_3 n \xi_n\} \exp\{-c_6 2^k\} \lesssim p \exp\{-c_5 c_3 \log(p \vee n)\} \\ &= \exp\{-c_5 c_3 \log(p \vee n) + \log p\} \leq p^{-c_6}, \end{aligned}$$

where c_6 can be chosen to be positive as long as we take $c_5 > 1/c_3$.

We complete the proof by noting that the remaining bound, (13), is implied by conditions (6) and C2, the derivations in the proof of Theorem 1 in [Radchenko & Mukherjee \(2014\)](#), and the aforementioned fact that all L_j and R_j lie in a bounded interval with high

probability.

The result of Corollary 1 follows from our Theorem 1 and Theorem 1 in Radchenko & Mukherjee (2014), due to the fact that the clustering scores, S_j , of the signal features are bounded away from zero.

6.4 Two stage approach to signal screening

We briefly describe the two stage approach to signal screening introduced in (Cai & Sun, 2016). We start with equation (4) where the estimated fdr has been obtained as

$$T_j = \widehat{\pi}_0 \widehat{f}_0(\psi_j) / \widehat{f}(\psi_j) \quad (15)$$

Order the estimated fdr's T_j from smallest to largest so that $T_{(1)} \leq T_{(2)} \leq \dots \leq T_{(p)}$. In the first stage, we estimate stage 1 screening cutoff k_s :

$$k_s = \min\{j : \sum_{i=p}^j (1 - T_{(i)}) \leq p(1 - \widehat{\pi}_0)\delta_p\} \quad (16)$$

with $\delta_p = \min(p, (\log p)^{-1})$ and select the features as

$$\mathcal{S}_s = \{j : T_j \leq T_{(k_s)}\} = \{T_{(1)}, \dots, T_{(k_s)}\} \quad (17)$$

In the second stage, the so-called *Discovery stage*, we take the stage 1 screened fdr's $\{T_j : j \in \mathcal{S}_s\}$ and estimate the stage 2 screening cutoff k_d :

$$k_d = \max\{1 \leq j \leq k_s : \frac{1}{j} \sum_{i=1}^j T_{(i)} \leq \delta_p\} \quad (18)$$

and select the features as

$$\widehat{\mathcal{L}}_S = \{j \in \mathcal{S}_s : T_j \leq T_{(k_d)}\} \quad (19)$$

Proposition 2 in Cai & Sun (2016) guarantees that in stage 1, \mathcal{S}_s is the largest subset such that the missed discovery rate (MDR) is controlled at level δ_p while in stage 2, $\widehat{\mathcal{L}}_S$ is the smallest subset such that the false positive rate (FPR) is controlled at level δ_p .

6.5 More real data examples

In Table 7, we present more real data examples to assess the performance of COSCI. We follow the theme presented in section 4.2 and overlay COSCI with k -means, Sparse k -means and IF-PCA for each of the eleven datasets considered below. The first ten data sets are sourced from Jiashun Jin’s webpage (see: <http://www.stat.cmu.edu/~jiashun/Research/software/GenomicsData/> and Table 1 in Jin & Wang (2014) for more information on these data sets.). The last data set is available on Brad Efron’s webpage (see: <http://statweb.stanford.edu/~ckirby/brad/LSI/datasets-and-programs/datasets.html>).

Table 7: Minimum CER of the competing methods alongwith the method name. For COSCI, the smallest CER observed for COSCI + ‘clustering method’ is shown where ‘clustering method’ includes the 5 competing methods in Table 5. Number of selected features are reported after the ‘/’ symbol.

Data Set	Source	n	p	K	Min. CER		COSCI	
					Method	CER	Min. CER	Method
ProstateCancer	Singh et al.(02)	102	6033	2	IF-PCA	0.477 / 1551	0.498 / 178	k-means
Lymphoma	Alizadeh et al.(00)	62	4026	3	IF-PCA	0.103 / 42	0.285 / 22	IF-PCA
Brain	Pomeroy et al.(02)	42	5597	5	IF-PCA	0.159 / 453	0.131 / 323	IF-PCA
Colon	Alon et al.(99)	62	2000	2	IF-PCA	0.490 / 25	0.444 / 3	k-means
SRBCT	Kahn(01)	63	2308	4	SAS	0.327 / 246	0.350 / 84	k-means
Leukemia	Golub et al.(99)	72	3571	2	IF-PCA	0.131 / 213	0.430 / 112	IF-PCA
SuCancer	Su et al.(01)	174	7909	2	SAS	0.501 / 526	0.500 / 211	k-means
LungCancer(1)	Gordon et al.(02)	181	12533	2	IF-PCA	0.064 / 251	0.206 / 420	k-means
LungCancer(2)	Bhattacharjee et al.(01)	203	12600	2	IF-PCA	0.341 / 418	0.502 / 260	k-means
BreastCancer	Wang et al.(05)	276	22215	2	IF-PCA	0.484 / 721	0.492 / 1195	k-means
Michigan	Subramanium et al.(05)	86	5217	2	Ex. Mass	0.427 / 4	0.479 / 51	k-means

IF-PCA returns a significantly smaller error rate on the Lymphoma, Leukemia and Lung Cancer datasets but barring these four datasets (Lymphoma, Leukemia, Lung Cancer (1) and Lung Cancer (2)), feature screening by COSCI returns comparable and often better error rates using fewer features when compared to the best competing method. The datasets of Breast Cancer and Michigan are the other exceptions where COSCI selects more features than the best competing method but still returns a comparable error rate.

6.6 Cardio Data and RNA Seq Data

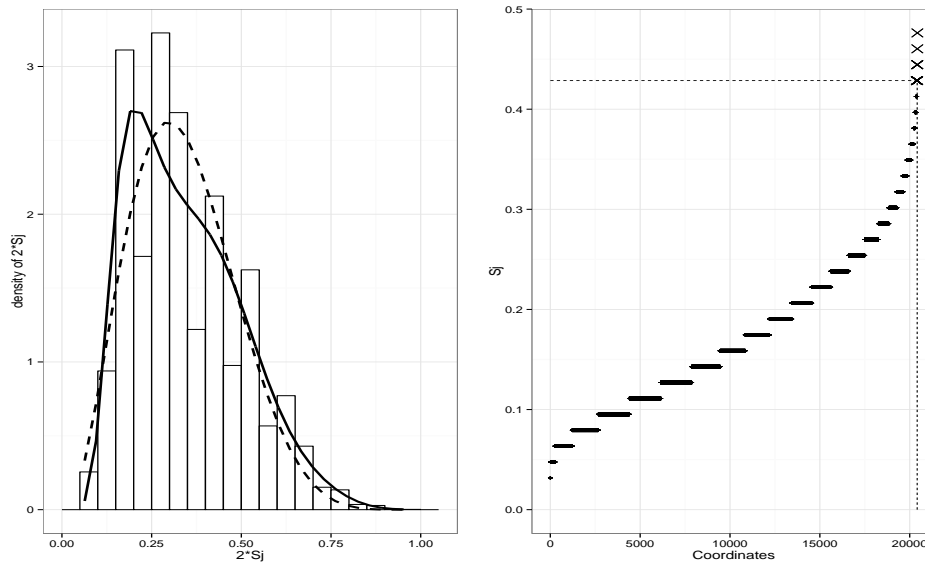


Figure 3: CARDIO DATA. Left: $\hat{\pi}_0 \hat{f}_0(\psi_j)$ in black dashed line and $\hat{f}(\psi_j)$ in black solid line for $j = 1, 2, \dots, 20426$. Right: Distribution of S_j . The 33 selected features are marked as \times . The dashed horizontal line is $\hat{\alpha}_0 = 0.428$.

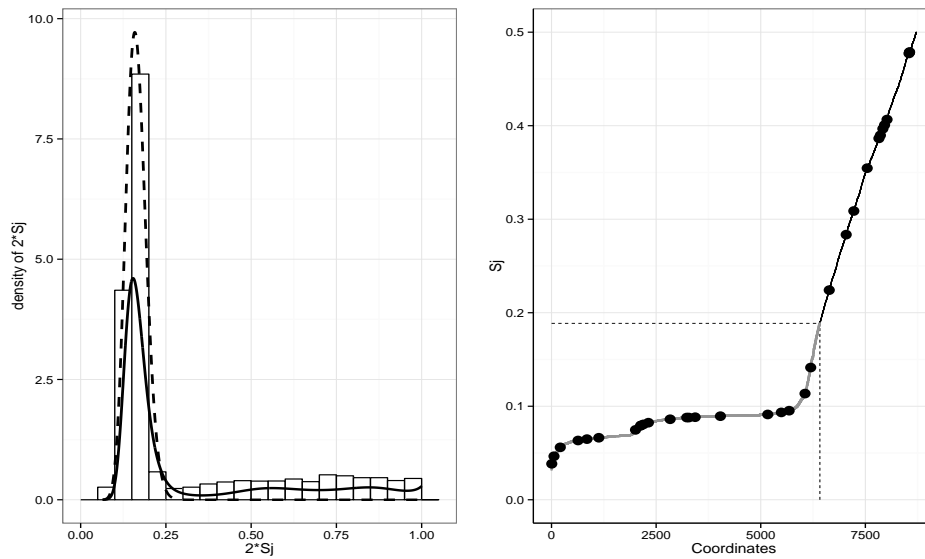


Figure 4: RNASEQ DATA. Left: $\hat{\pi}_0 \hat{f}_0(\psi_j)$ in black dashed line and $\hat{f}(\psi_j)$ in black solid line for $j = 1, 2, \dots, 8716$. Right: Distribution of S_j . The dashed horizontal line is $\hat{\alpha}_0 = 0.188$. The 2304 selected features are in black and are above the dashed horizontal line. The black dots are the 33 lineage markers.

6.7 Estimation of Hyperparameters - simulation based

Table 8: This table reports the % of cases where COSCI detects clusters across varying sample sizes n and thresholds α_0 .

		α_0						
Unimodal density	n	0.01	0.02	0.05	0.1	0.15	0.2	0.25
N(0,1)	100	100	100	99	74	47	28	12
	500	100	100	67	33	17	11	7
	1000	100	98	49	22	13	6	2
	2000	100	82	21	10	3	0	0
	5000	94	38	3	1	1	0	0
	10000	47	6	0	0	0	0	0
t with 1 df	100	100	100	59	19	11	3	1
	500	99	50	4	0	0	0	0
	1000	74	14	0	0	0	0	0
	2000	27	0	0	0	0	0	0
	5000	0	0	0	0	0	0	0
	10000	0	0	0	0	0	0	0
Exp(1)	100	100	100	96	59	33	14	7
	500	100	99	47	10	2	2	0
	1000	100	84	7	2	0	0	0
	2000	95	33	0	0	0	0	0
	5000	35	0	0	0	0	0	0
	10000	2	0	0	0	0	0	0
Cauchy	100	100	99	52	18	10	2	1
	500	99	62	7	1	0	0	0
	1000	82	17	0	0	0	0	0
	2000	36	3	0	0	0	0	0
	5000	0	0	0	0	0	0	0
	10000	0	0	0	0	0	0	0
Double Exponential(1)	100	100	100	75	29	13	2	1
	500	100	81	11	1	0	0	0
	1000	98	40	1	0	0	0	0
	2000	71	8	0	0	0	0	0
	5000	4	0	0	0	0	0	0
	10000	0	0	0	0	0	0	0
GEV with shape parameter = 0.8	100	100	100	80	28	16	7	2
	500	100	82	15	3	0	0	0
	1000	99	48	3	0	0	0	0
	2000	68	12	0	0	0	0	0
	5000	13	0	0	0	0	0	0
	10000	0	0	0	0	0	0	0
Beta with parameters = 1, 3	100	100	100	99	78	50	32	19
	500	100	100	74	28	16	11	2
	1000	100	98	37	5	3	1	0
	2000	99	80	14	2	0	0	0
	5000	88	24	2	0	0	0	0
	10000	43	1	0	0	0	0	0
Triangle distbn. $\in [0, 1]$ with mode at 0.8	100	100	100	99	84	54	33	22
	500	100	100	79	34	15	7	0
	1000	100	98	42	11	4	4	1
	2000	100	88	28	5	1	0	0
	5000	98	40	3	0	0	0	0
	10000	68	11	0	0	0	0	0

6.8 Detailed description of Algorithm 1

input: data matrix $X^{n \times p}$ and tuning parameter α_0

output: merge sizes $\{S_j\}_1^p$ for p features and feature set $\widehat{\mathcal{L}}_S$

FOR each $j \in \{1, 2, \dots, p\}$

 INITIALIZE;

$k =$ number of clusters $= n$

 sort $x = \{x_1, \dots, x_n\}$ in ascending order

 assign cluster mean: $a_i = x_i$ for $i = 1, \dots, n$

 assign cluster size: $s_i = 1, i = 1, \dots, n$

 assign cluster membership indices of x : $I(x) = \{1, \dots, n\}$

 WHILE $k > 1$

Convex Merging Algorithm

 /* 1. find the consecutive adjacent centroid distances */

$d(r, r+1) \leftarrow (a_{r+1} - a_r)/(s_r + s_{r+1})$

 /* 2. find clusters with minimum merging distance */

$r^* \leftarrow \arg \min_{1 \leq r \leq k-1} d(r, r+1)$

Merge Sizes

 /* 3. determine merge size α_i^j */

$\alpha_i^j = n^{-1} \min\{s_{r^*}, s_{r^*+1}\}, i = \text{merge index}$

Screening the Merges

 /* 4. obtain mass after merge m_i */

$m_i = n^{-1} (s_{r^*} + s_{r^*+1})$

 IF $m_i < 0.5$ then $\alpha_i^j = 0$

Prepare for the next iteration

 /* 5. merge r^*, r^*+1 clusters */

$a_{r^*} \leftarrow (s_{r^*} a_{r^*} + s_{r^*+1} a_{r^*+1}) / (s_{r^*} + s_{r^*+1})$

$s_{r^*} \leftarrow s_{r^*} + s_{r^*+1}$

 /* 6. reduce number of clusters */

$k \leftarrow k - 1$

 /* 7. change cluster and member indices */

 FOR l in $(r^* + 1) : k, s_l \leftarrow s_{l+1}, a_l \leftarrow a_{l+1}$

 FOR ALL $I(x) > r^*$: $I(x) = I(x) - 1$

Store max merge sizes

 store $S_j = \max_{1 \leq i \leq (n-1)} \alpha_i^j$

Feature screening

Choose $\widehat{\mathcal{L}}_S = \{j : S_j \geq \alpha_0\}$

Algorithm 1: COSCI procedure for feature screening.

References

- AMIR, E.-A. D., DAVIS, K. L., TADMOR, M. D., SIMONDS, E. F., LEVINE, J. H., BENDALL, S. C., SHENFELD, D. K., KRISHNASWAMY, S., NOLAN, G. P. & PE'ER, D. (2013). visne enables visualization of high dimensional single-cell data and reveals phenotypic heterogeneity of leukemia. *Nature biotechnology* **31**, 545–552.
- ARIAS-CASTRO, E. & PU, X. (2016). A simple approach to sparse clustering. *arXiv preprint arXiv:1602.07277* .
- ARIAS-CASTRO, E. & VERZELEN, N. (2014). Detection and feature selection in sparse mixture models. *arXiv preprint arXiv:1405.1478* .
- AZIZYAN, M., SINGH, A. & WASSERMAN, L. (2013). Minimax theory for high-dimensional gaussian mixtures with sparse mean separation. In *Advances in Neural Information Processing Systems*.
- BENDALL, S. C., DAVIS, K. L., AMIR, E.-A. D., TADMOR, M. D., SIMONDS, E. F., CHEN, T. J., SHENFELD, D. K., NOLAN, G. P. & PEER, D. (2014). Single-cell trajectory detection uncovers progression and regulatory coordination in human b cell development. *Cell* **157**, 714–725.
- BENDALL, S. C., SIMONDS, E. F., QIU, P., AMIR, E. D., KRUTZIK, P. O., FINCK, R., BRUGGNER, R. V., MELAMED, R., TREJO, A., ORNATSKY, O. I., BALDERAS, R. S., PLEVritis, S. K., SACHS, K., PE'ER, D., TANNER, S. D. & NOLAN, G. P. (2011). Single-cell mass cytometry of differential immune and drug responses across a human hematopoietic continuum. *Science* .
- BENJAMINI, Y. & HOCHBERG, Y. (1995). Controlling the false discovery rate: a practical and powerful approach to multiple testing. *Journal of the royal statistical society. Series B (Methodological)* , 289–300.
- BONDELL, H. D. & REICH, B. J. (2008). Simultaneous regression shrinkage, variable selection, and supervised clustering of predictors with oscar. *Biometrics* **64**, 115–123.
- CAI, T. & SUN, W. (2016). Optimal screening and discovery of sparse signals with applications to multistage high throughput studies. *Journal of the Royal Statistical Society: Series B (Statistical Methodology)* .

- CHAN, Y.-B. & HALL, P. (2012). Using evidence of mixed populations to select variables for clustering very high-dimensional data. *Journal of the American Statistical Association* .
- CHANG, W.-C. (1983). On using principal components before separating a mixture of two multivariate normal distributions. *Applied Statistics* , 267–275.
- CHENG, M.-Y. & HALL, P. (1998). Calibrating the excess mass and dip tests of modality. *Journal of the Royal Statistical Society: Series B (Statistical Methodology)* **60**, 579–589.
- CHI, E. C. & LANGE, K. (2015). Splitting methods for convex clustering. *Journal of Computational and Graphical Statistics* **24**, 994–1013.
- CHIPMAN, H. & TIBSHIRANI, R. (2006). Hybrid hierarchical clustering with applications to microarray data. *Biostatistics* **7**, 286–301.
- DALERBA, P., KALISKY, T., SAHOO, D., RAJENDRAN, P. S., ROTHENBERG, M. E., LEYRAT, A. A., SIM, S., OKAMOTO, J., JOHNSTON, D. M., QIAN, D. et al. (2011). Single-cell dissection of transcriptional heterogeneity in human colon tumors. *Nature biotechnology* **29**, 1120–1127.
- DONOHO, D. & JIN, J. (2004). Higher criticism for detecting sparse heterogeneous mixtures. *Annals of Statistics* , 962–994.
- DONOHO, D. & JIN, J. (2008). Higher criticism thresholding: Optimal feature selection when useful features are rare and weak. *Proceedings of the National Academy of Sciences* **105**, 14790–14795.
- EFRON, B. (2007). Size, power and false discovery rates. *The Annals of Statistics* , 1351–1377.
- EFRON, B., TIBSHIRANI, R. et al. (1996). Using specially designed exponential families for density estimation. *The Annals of Statistics* **24**, 2431–2461.
- FARCOMENI, A. & GRECO, L. (2016). *Robust methods for data reduction*. CRC press.
- FRIEDMAN, J., HASTIE, T. & TIBSHIRANI, R. (2001). *The elements of statistical learning*, vol. 1. Springer series in statistics Springer, Berlin.

- FRIEDMAN, J. H. & MEULMAN, J. J. (2004). Clustering objects on subsets of attributes (with discussion). *Journal of the Royal Statistical Society: Series B (Statistical Methodology)* **66**, 815–849.
- GIECOLD, G., MARCO, E., GARCIA, S. P., TRIPPA, L. & YUAN, G.-C. (2016). Robust lineage reconstruction from high-dimensional single-cell data. *Nucleic acids research*, gkw452.
- HARTIGAN, J. (1987). Estimation of a convex density contour in two dimensions. *Journal of the American Statistical Association* **82**, 267–270.
- HARTIGAN, J. A. & HARTIGAN, P. (1985). The dip test of unimodality. *The Annals of Statistics*, 70–84.
- HARTIGAN, J. A. & WONG, M. A. (1979). Algorithm as 136: A k-means clustering algorithm. *Journal of the Royal Statistical Society. Series C (Applied Statistics)* **28**, 100–108.
- HOCHREITER, S., BODENHOFER, U., HEUSEL, M., MAYR, A., MITTERECKER, A., KASIM, A., KHAMIKOVA, T., VAN SANDEN, S., LIN, D., TALLOEN, W., BIJNENS, L., G’OHLMANN, H. W. H., SHKEDY, Z. & CLEVERT, D.-A. (2010). FABIA: Factor analysis for bicluster acquisition. *Bioinformatics* **26**, 1520–1527. Doi:10.1093/bioinformatics/btq227.
- HOCKING, T. D., JOULIN, A., BACH, F. & VERT, J.-P. (2011). Clusterpath an algorithm for clustering using convex fusion penalties. In *28th international conference on machine learning*.
- HOEFLING, H. (2010). A path algorithm for the fused lasso signal approximator. *Journal of Computational and Graphical Statistics* **19**, 984–1006.
- JAMES, G., WITTEN, D., HASTIE, T. & TIBSHIRANI, R. (2013). *An introduction to statistical learning*, vol. 6. Springer.
- JIN, J., KE, Z. T. & WANG, W. (2015). Phase transitions for high dimensional clustering and related problems. *arXiv preprint arXiv:1502.06952*.

- JIN, J. & WANG, W. (2014). Important feature pca for high dimensional clustering. *arXiv preprint arXiv:1407.5241* .
- JOHNSTONE, I. M. & LU, A. Y. (2009). On consistency and sparsity for principal components analysis in high dimensions. *Journal of the American Statistical Association* **104**, 682693.
- KE, T., FAN, J. & WU, Y. (2013). Homogeneity in regression. *arXiv preprint arXiv:1303.7409* .
- LINDSEY, J. (1974). Construction and comparison of statistical models. *Journal of the Royal Statistical Society. Series B (Methodological)* , 418–425.
- LIU, L., LI, Y., LI, S., HU, N., HE, Y., PONG, R., LIN, D., LU, L. & LAW, M. (2012). Comparison of next-generation sequencing systems. *BioMed Research International* **2012**.
- PAN, W. & SHEN, X. (2007). Penalized model-based clustering with application to variable selection. *Journal of Machine Learning Research* **8**, 1145–1164.
- PAUL, F., ARKIN, Y., GILADI, A., JAITIN, D. A., KENIGSBURG, E., KEREN-SHAUL, H., WINTER, D., LARA-ASTIASO, D., GURY, M., WEINER, A. et al. (2015). Transcriptional heterogeneity and lineage commitment in myeloid progenitors. *Cell* **163**, 1663–1677.
- QIU, P., SIMONDS, E. F., BENDALL, S. C., GIBBS JR, K. D., BRUGGNER, R. V., LINDERMAN, M. D., SACHS, K., NOLAN, G. P. & PLEVRETTIS, S. K. (2011). Extracting a cellular hierarchy from high-dimensional cytometry data with spade. *Nature biotechnology* **29**, 886–891.
- RADCHENKO, P. & MUKHERJEE, G. (2014). Convex clustering via l_1 fusion penalization. *Journal of the Royal Statistical Society. Series B (forthcoming)*; *arXiv preprint arXiv:1412.0753* .
- RAND, W. M. (1971). Objective criteria for the evaluation of clustering methods. *Journal of the American Statistical association* **66**, 846–850.

- ROUSSEEUW, P. J. & KAUFMAN, L. (1990). *Finding Groups in Data*. Wiley Online Library.
- SEN, N., MUKHERJEE, G. & ARVIN, A. M. (2015). Single cell mass cytometry reveals remodeling of human t cell phenotypes by varicella zoster virus. *Methods* **90**, 85–94.
- SHEN, X. & HUANG, H.-C. (2010). Grouping pursuit through a regularization solution surface. *Journal of the American Statistical Association* **105**.
- SHEN, X., HUANG, H.-C. & PAN, W. (2012). Simultaneous supervised clustering and feature selection over a graph. *Biometrika* **99**, 899–914.
- SPITZER, M. H., GHERARDINI, P. F., FRAGIADAKIS, G. K., BHATTACHARYA, N., YUAN, R. T., HOTSON, A. N., FINCK, R., CARMİ, Y., ZUNDER, E. R., FANTL, W. J. et al. (2015). An interactive reference framework for modeling a dynamic immune system. *Science* **349**, 1259425.
- SU, A. I., COOKE, M. P., CHING, K. A., HAKAK, Y., WALKER, J. R., WILTSHIRE, T., ORTH, A. P., VEGA, R. G., SAPINOSO, L. M., MOQRICH, A. et al. (2002). Large-scale analysis of the human and mouse transcriptomes. *Proceedings of the National Academy of Sciences* **99**, 4465–4470.
- TAN, K. M. & WITTEN, D. (2015). Statistical properties of convex clustering. *arXiv preprint arXiv:1503.08340*.
- VAN DER VAART, A. & WELLNER, J. (1996). Weak convergence and empirical processes with applications to statistics.
- WANG, D. & BODOVITZ, S. (2010). Single cell analysis: the new frontier in omics. *Trends in biotechnology* **28**, 281–290.
- WANG, S. & ZHU, J. (2008). Variable selection for model-based high-dimensional clustering and its application to microarray data. *Biometrics* **64**, 440–448.
- WHITE, A. K., VANINSBERGHE, M., PETRIV, I., HAMIDI, M., SIKORSKI, D., MARRA, M. A., PIRET, J., APARICIO, S. & HANSEN, C. L. (2011). High-throughput microfluidic single-cell rt-qpcr. *Proceedings of the National Academy of Sciences* **108**, 13999–14004.

- WITTEN, D. M. & TIBSHIRANI, R. (2012). A framework for feature selection in clustering. *Journal of the American Statistical Association* .
- XIE, B., PAN, W. & SHEN, X. (2008). Penalized model-based clustering with cluster-specific diagonal covariance matrices and grouped variables. *Electronic journal of statistics* **2**, 168.
- ZHU, C., XU, H., LENG, C. & YAN, S. (2014). Convex optimization procedure for clustering: Theoretical revisit. In *Advances in Neural Information Processing Systems*.